Photothermal reflectance investigation of processed silicon. II. Signal generation and lattice temperature dependence in ion-implanted and amorphous thin layers

I. Alex Vitkin, Constantinos Christofides, and Andreas Mandelis
Photoacoustic and Photothermal Sciences Laboratory, Department of Mechanical Engineering and Ontario Laser and Lightwave Research Center, University of Toronto, Toronto, Ontario M5S 1A4, Canada

(Received 3 April 1989; accepted for publication 1 December 1989)

Photothermal reflectance investigations as a function of temperature of various forms of silicon (crystalline, ion-implanted, amorphous) are reported largely in the thermal wave regime (low-modulation frequencies and large laser beam spot sizes). The observed results have been explained by a thermal wave model that has been extended to include the effect of lattice temperature. The influence of substrate on the observed signal has been examined in light of the temperature and frequency dependence of the thermal diffusion length. The possible application of the technique to depth-profiling studies, and to the investigation of ion-implanted semiconductors, is discussed.

I. INTRODUCTION

During the last few years, photothermal wave physics has been successfully applied to the investigation of semiconductor properties. The noncontact character of the associated techniques makes them particularly attractive for the nondestructive evaluation of materials. Some of the noncontact methods that employ optical excitation include (i) modulated thermoreflectance or photothermal reflectance (PTR), which is able to detect the local variations in the reflectivity of the material[1]; (ii) photothermal deflectometry, which allows measurements of the induced thermoelastic deformation of the surface[2,3]; (iii) photothermal beam deflection, which samples the refractive index gradient in the specimen or above its surface[4]; and (iv) photothermal radiometry, which allows the measurement of the optically induced emission of the blackbody radiation of the surface.[5,6]

The photothermal reflectance technique has recently been employed as a method for characterizing silicon damaged by ion implantation.[7-10] However, all of the previous studies have been performed at room temperature. In this work, we present some results extending the conventional laser-induced PTR method to low temperatures ($\approx$20 K). Such measurements allow the estimation of certain important characteristics such as the local electronic and thermal transport parameters, which, in the case of implanted semiconductors, provide an indication of the local degree of damage. Considering the significant amount of information provided by the PTR-T (temperature) method, such studies are expected to be very fruitful with regard to the understanding of the underlying physics of the optical and thermal phenomena in semiconductors.

The aim of this paper is to present and interpret new results concerning the temperature dependence of the photothermal signal in silicon. Towards this end, PTR measurements as a function of temperature (T: 20–300 K) and modulation frequency (f: 3–4000 kHz) have been conducted on different silicon samples: p-type crystalline wafers, arsenic- and phosphorus-implanted (annealed and nonannealed) layers, and amorphous films deposited on a crystalline silicon substrate. Such a study will complement the room-temperature PTR investigation reported in the companion paper.[9] The variety of samples and the choice of the experimental parameters will allow us to vary the relative contributions of the thermal wave and the plasma wave mechanisms that give rise to the measured signal. As was discussed in part I,[9] the present studies were performed in the PTR thermal wave regime (relatively low-modulation frequencies and defocused laser beams). As will be shown below by a model that incorporates the temperature dependencies of material parameters, the observed experimental trends corroborate, and can be satisfactorily explained in terms of, the thermal wave picture alone. In addition, the influence of temperature and the modulation frequency on the thermal diffusion length will be discussed.

II. THEORY

The mechanism of PTR signal generation in semiconductors can be understood in terms of the induced modulation of the refractive index. Generally, there are two (coupled) contributions to the modulation, due to the excursions in the local sample temperature (thermal-wave effect) and due to the photo-induced changes in the free-carrier density (plasma-wave effect).[11-13] We can express the total PTR signal, $\Delta R/R_0$, as

$$\frac{\Delta R}{R_0}=\frac{\Delta R_{\rm th}}{R_0}+\frac{\Delta R_{\rm pl}}{R_0}, \tag{1a}$$

where $\Delta R_{\rm th}$ and $\Delta R_{\rm pl}$ are the photothermal signal components due to the thermal and plasma effect, respectively, and R_0 is the reflectivity at temperature T_0 and plasma density N_0. Quantitatively, Eq. (1a) can be written as[10]

$$\frac{\Delta R}{R_0}=\frac{1}{R_0}\left(\frac{\partial R}{\partial T}\right)\Delta T+\frac{1}{R_0}\left(\frac{\partial R}{\partial N}\right)\Delta N, \tag{1b}$$

 0021-8979/90/062822-09$03.00

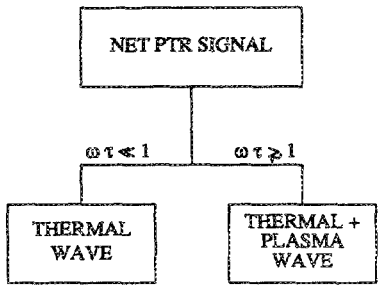

FIG. 1. Flowchart of the PTR-T signal components.

where $1/R_0(\partial R/\partial T)$ and $1/R_0(\partial R/\partial N)$ are the temperature and the plasma coefficients of reflectivity (the latter can be negative) and ΔR, ΔT, and ΔN are the local variations in the reflectance, temperature, and plasma density, respectively, brought about by the heating laser. The relative importance of the two mechanisms is determined by the $\omega\times\tau$ product, where $\omega = 2\pi f$ is the angular modulation frequency, and τ is the lifetime of the excess free carriers. The situation is described schematically in Fig. 1. Essentially, the value of $\omega\times\tau$ specifies the ratio of the relaxation to the detection time in a given cycle. Thus, when the product is much less than unity, the plasma has thermalized with the lattice (the excess carriers have decayed) and the detector is measuring the change in reflectivity due to the local temperature rise. On the other hand, when $\omega\times\tau > 1$, the generated carriers exist long enough to be detected, and the plasma contribution may become comparable to the thermal contribution, or even dominate it. In our experiments, the situation is somewhat complicated because the relaxation time is a decreasing function of temperature[14]:

$$\tau(T) = 1/\alpha_r d_0(T), \tag{2}$$

where α_r is a constant or proportionality which depends on the particular mechanism by which recombination takes place, and d_0 is the equilibrium carrier concentration, which increases with temperature. Thus, lowering the experimental temperature increases the $\omega\times\tau$ product at a given modulation frequency. Typical room-temperature values of the relaxation time are $\tau \approx 10^{-6}$ s for c-Si,[11,14] and several orders of magnitude lower for damaged or amorphous layers.[15] Hence, for example, at the experimental frequency of 100 kHz, we expect to be largely in the thermal regime for ion-implanted silicon (at all measurement temperatures) and to be in the combined thermal/plasma regime for the crystalline wafer. To ensure thermal wave behavior for the crystalline sample, additional studies at a lower modulation frequency $f = 3$ kHz were performed, thus limiting the plasma contribution to the plasma/lattice thermalization mechanism. Similar approaches were previously discussed by Guidotti and van Driel.[16]

In the ensuing analysis, we present a quantitative theoretical approach[17,18] that we extend to include the effect of measurement temperature. In this model, the contribution from photoinduced plasma was not included, and the temperature effects are explained solely in terms of the thermal-wave T dependence of modulated reflectance. In general, this first-order approximation is not expected to be strictly adequate at low temperatures or at high-modulation frequencies, but most of the trends in our data can be adequately described by the temperature dependence of the thermal wave term alone (see also Ref. 16). Additional work is underway to determine the extent to which the plasma wave term is playing a role in our measurements, and whether its temperature dependence in different silicon environments may be experimentally decoupled from that of the purely thermal wave contribution.

To evaluate the thermoreflectance component of the PTR signal, we follow the derivation given by Wetsel,[17] and Doka, Mikos, and Lorincz.[18] In this one-dimensional (x) formulation, the specimen is assumed to behave as a semi-infinite medium with a stress-free boundary and a surface heat source of density h, at $x=0$ (which is brought in as a boundary condition). The solution of the coupled thermal diffusion and elastic-wave equations yields an expression for $T(x,t)$, where t is the time. In applying this solution to our particular experiment, we follow the development given by Doka and co-workers.[18] There, it is shown that the photothermal signal will be proportional to the variations in the surface temperature $T(0,t)$, whose steady-state level is equal to the temperature in our experimental chamber. The resultant signal amplitude may be written as

$$\frac{\Delta R_{\rm th}(T)}{R_0} \approx g(n,\kappa,v,w)\frac{h}{\sqrt{(\omega\rho Ck)}}, \tag{3}$$

where ρ is the density of the solid, C is the specific heat at constant volume, and k is the thermal conductivity. $g(n,\kappa,v,w)$ is an essentially temperature-independent factor which is a function of the real and the imaginary parts of the refractive index of the medium (n,κ) at a reference temperature, and of the total temperature derivatives of the real and imaginary parts of the dielectric constant (v,w). We note in Eq. (3) that the signal is inversely proportional to the square root of angular frequency. It is also inversely proportional to the sample thermal effusivity (which is a function of temperature). This latter fact will largely dictate the temperature dependence of the thermal wave component of the PTR-T signal, as the refractive index components and their derivatives are expected to exhibit only weak T dependencies.

The effect of the photogenerated plasma, which becomes important for $\omega\tau > 1$, has been studied by several workers.[11,12] Assuming a spatially homogeneous e-h plasma, and a simple Drude effect model, the plasma reflectance term gives

$$\frac{\Delta R_{\rm pl}(T)}{R_0} = -\frac{2\lambda^2 e^2}{\pi m^* v_c^2}\frac{\Delta N}{n(n^2-1)}, \tag{4}$$

where e is the electron charge, m^* is the electron's effective

mass, v_c is the velocity of light, and λ is the optical wavelength of the probe laser. The temperature-varying parameters in the above expression are the real part of the refractive index, n, and the excess plasma density, ΔN (we ignore the small change in the effective mass which arises because of the slight shift of the silicon's energy levels with temperature). As a result, the term $[n(n^2-1)]^{-1}$ is about 10% greater at 20 K than at 300 K.[19] The temperature dependence of the ΔN term is more difficult to quantify because of the complex temperature dependence of the ambipolar diffusion coefficient. As mentioned previously, this (changing) contribution will be noticeable only at $\omega\times\tau$ values close to or greater than unity. The product itself will change because the relaxation lifetime decreases with temperature [see Eq. (2)]. Thus, the plasma effect, if detectable at all, will be seen in a crystalline material, at low temperatures, and at our highest experimental modulation frequency. So, to first order, we neglect it for $f\leqslant 100$ kHz, without introducing a substantial error.[16]

III. EXPERIMENT

A. Silicon samples

For this study, three families of samples have been used (see companion paper[9] for a more detailed description):

(i) 2-in.-diam silicon n-type (100) wafers were implanted at room temperature with phosphorus (dose $\Phi = 1\times10^{12}$ to 1×10^{16} ions/cm^2; energy $E = 150$ keV). Some of these samples have been annealed at 1100 °C for 15 min.

(2) 2-in.-diam silicon p-type (100) wafers were implanted at room temperature with arsenic ($\Phi = 2\times10^{14}$ or 5×10^{14} ions/cm^2; $E = 150$ keV). Some of these samples were then thermally annealed (between 400 and 800 °C for 1 h) in an inert nitrogen atmosphere.

(3) Amorphous silicon (a-Si) deposited on crystalline silicon substrate, with approximate layer thickness $L_{a\text{-Si}} \approx 0.15\ \mu$m.

B. Experimental setup

The block diagram of the experimental apparatus has been presented in the companion paper,[9] where the room-temperature operation of the system was thoroughly described. Briefly, the measured signal was the change in reflectivity of the probe beam (633 nm line of the HeNe laser), brought about by the synchronous modulation of the heating pump beam (488 nm line of the Ar^+ laser). Both beams were focussed normally onto the silicon surface to a spot size of about 30 μm. To perform a temperature study, the semiconductor wafer was placed in the experimental chamber of a helium-cooled expander module (APD Cryogenics Model PS2). Optical access was available through a vacuum-sealed quartz window. The operating pressures within the chamber, obtained with a GE mechanical pump (Model D2A), and measured with a Thermovac Pirani gauge (TM 200), were 10^{-3}–10^{-5} Torr. The experimental temperature range, as monitored by a gold/iron: constantan thermocouple with 0.1 K accuracy, was 20–300 K. As the chamber temperature was lowered at a rate of 2.5 K min^{-1}, the thermocouple voltage was periodically probed by the computer. Once the voltage change corresponded to a temperature difference of 1 K, several data points from the fast lock-in amplifier (EG&G 5202) were recorded and averaged. Thus, the in-phase and the quadrature components of the photodetector output, and the corresponding chamber temperature, were stored in the computer at regular 1 K intervals. The frequency studies were performed by changing the sinusoidal output of the signal generator (Dynascan 3025). The output frequency was measured with a Fluke 1910A frequency meter, to an accuracy of 0.01%.

IV. RESULTS AND DISCUSSION

In this section we will present our experimental results and will provide some qualitative and semiquantitive interpretations. The photothermal reflectance signal [see Eqs. (1a) and (1b)] will be analyzed as a function of the measurement temperature and the modulation frequency. The complex character of implanted semiconductor layers, which seem to behave both as an inhomogeneous material (crystalline matrix with isolated damaged regions-clusters, defects, dislocation lines and loops, etc.)[20] and, on the other hand, as an amorphous material, has led us to compare the implanted layers with crystalline c-Si and amorphous a-Si. In addition, these limiting cases facilitate in understanding the mechanism(s) responsible for our experimental data, because of their opposite temperature dependence of the thermal conductivity parameter.[21] Thus, the temperature-dependent photothermal signal of the implanted (annealed and nonannealed), amorphous, and crystalline layers will be discussed in light of the theoretical model presented in Sec. II. A qualitative discussion of the ion-implantation-induced damage, and its effect on the PTR-T signal, will also be given.

A. Preliminary results

Before attempting to interpret our PTR-T data, we present some preliminary results that are characteristic of our technique, and that address some experimental observations pointed out by other workers in the field.[7,8,11,12] First, our PTR signal is simply the change in modulated reflectance, ΔR, and not the normalized reflectance signal, $\Delta R/R_0$ (R_0 is the dc reflectivity). This is simply a matter of convenience, as the dc reflectivity of silicon varies very little with lattice temperature. Quantitatively, for normal incidence,

$$R_0 = R(n_0,\kappa_0) = \frac{(n_0-1)^2+\kappa_0^2}{(n_0+1)^2+\kappa_0^2}, \tag{5}$$

where κ_0 is related to the optical absorption coefficient through $\alpha = 4\pi\kappa_0/\lambda$. At room temperature and at the HeNe laser wavelength ($\lambda = 633$ nm), $n_0 = 3.89$ and $\kappa_0 = 1.51\times10^{-2}$, giving R_0 (300 K) = 34.93%. At 77 K, the optical parameters are $n_0 = 3.83$ and $\kappa_0 = 5.04\times10^{-3}$, thus R_0(77 K) = 34.33%.[19,22] For experimental verification, a one-beam

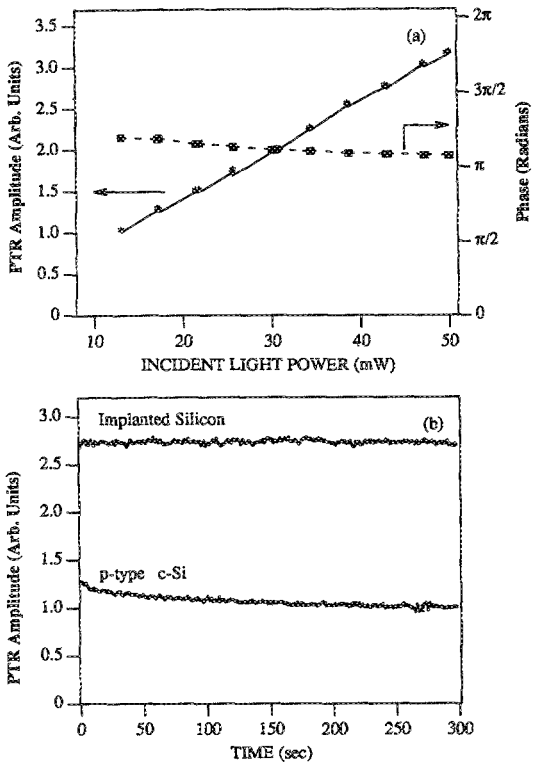

FIG. 2. (a) PTR signal as a function of the incident light power. (b) Temporal dependence of the photothermal signal.

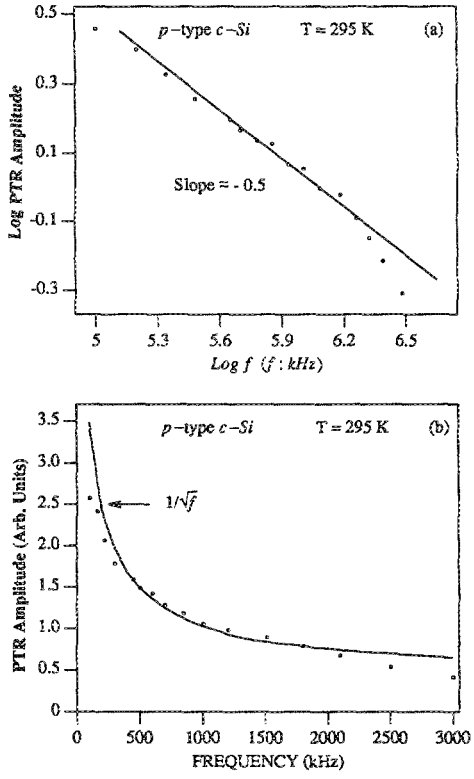

FIG. 3. (a) Logarithmic plot of the photothermal reflectance signal as a function of modulation frequency for p-type c-Si. (b) Same data on a linear scale (to obtain the value of H_T). Solid curve: $1/\sqrt{f}$ theoretical fitting; points; experimental results.

reflectivity experiment was performed throughout the 20–300 K temperature range, and the signal was essentially constant. Clearly, the small changes in dc reflectivity are not sufficient to account for the large PTR-T signal variations presented later, and the R_0 contribution was thus ignored.

To ensure the linearity of the PTR signal with the incident pump beam power, a p-type silicon wafer was examined under different heating laser (Ar^+) outputs. The magnitude of the resultant signal as function of incident light power at the sample (measured with a Coherent 210 power meter) is indeed linear, and the phase is essentially intensity independent, as expected [Fig. 2(a)]. All subsequent experiments were thus performed in this linear power range, mostly at 25 mW.

The temporal decay of the modulated PTR signal has been recently reported,[11,12] and has been explained in terms of electron-hole plasma/electronic surface states interaction. We also observe a slight signal decrease for the crystalline p-type silicon (at room temperature). By the time a steady signal is reached (typically 5 min), this decrease would amount to approximately 15% of the initial signal, as demonstrated in Fig. 2(b). Also shown is the signal of the phosphorus-implanted Si ($\Phi = 10^{16}$ ions/cm^2) where no time decay is observed. In fact, none of the as-implanted, implanted and annealed, or the amorphous samples showed any signs of temporal decay. To ensure consistency and ease of comparison with the p-type crystalline wafer, the data for this sample were taken after 5 min of continuous focusing, in order to account for any temporal decrease of the signal.

B. Temperature and frequency dependence of the PTR signal

We are now in a position to compare the theoretical predictions of Sec. II with experimental results. From Eq. (3), the expected frequency dependence of the thermal wave PTR signal is $\Delta R_{\rm th} \propto 1/\sqrt{f}$. The log-log plot of the experimental data for p-type c-Si, displayed in Fig. 3(a), reveals that the power exponent is indeed close to -0.5. There is a slight departure from the straight line dependence at high frequencies (>1 MHz), likely related to the temporal response of the detection instrumentation. Nevertheless, the $1/\sqrt{f}$ thermal-wave behavior is evident for the range of frequencies where it is expected to be the dominant effect. Figure 3(b) shows the same data on a linear scale; a good agreement between the experimental points and the theoretical fitting (solid curve) as $1/\sqrt{f}$ can be seen, implying consistency with the underlying theory in the range below 2.5 MHz. For this fitting, the frequency-independent constant, H_T [$H_T = g(n,\kappa,v,w)h/\sqrt{2\pi\rho Ck}$] has been taken equal to 3.6×10^{-4}. Thus, one may, in principle, employ the PTR measurements as a function of frequency (in the range where thermal effects dominate) at different temperatures to evaluate some otherwise elusive sample parameters, such as the temperature derivatives of

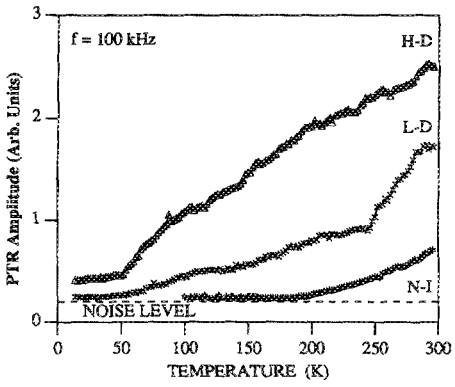

FIG. 4. PTR signal vs temperature for samples implanted at two different doses [low dose (LD): 2×10^{14} As^+/cm^2 and high dose (HD): 5×10^{14} As^+/cm^2] and for nonimplanted (N-I) p-type reference sample.

the dielectric constant, v and w [note that they were assumed to be temperature independent in the theoretical derivation leading to Eq. (3); this presents a method to test the assumption]. In fact, by performing the frequency measurements under the same optical conditions (same diameter of the light spot, same power, etc., so as to keep h constant) at different temperatures, it will be possible to generate a set of $H_T(T)$ values by a $1/\sqrt{f}$ fitting, and then extract information about the magnitudes of the various parameters contained in H_T.

The PTR-T signal of the c-Si sample presented in Fig. 3 may contain a plasma-wave component, as discussed previously. To circumvent this possible complication, heavily damaged implanted silicon was also studied as a function of frequency ($\Phi = 10^{15}$ As^+/cm^2). The result again closely followed the inverse square root dependence, with a slight departure at high frequencies due to the same instrumental factors as in Fig. 3 above, but with a different value of H_T. This behavior of the layer with a shorter τ implies that the $1/\sqrt{f}$ dependence indeed arises from the thermal-wave component of the PTR signal, in accordance with the theory derived in Sec. II.

Figure 4 shows the variation of the PTR signal with temperature for two different arsenic ion doses, ($2\times$ and 5×10^{14} ions/cm^2) as well as for one nonimplanted p-type crystalline wafer which was used as a reference. A higher signal was observed for the high-doping-level sample at all temperatures, which is consistent with the higher degree of lattice damage caused by the implant.[23,24] Before we discuss the effects responsible for the signal increase with temperature, it is worth noting that the difference in the room-temperature amplitudes reveals a doping-level sensitivity which is somewhat inferior to the sensitivity reported by other authors[24–26] working in the plasma-wave regime. This is so because the present measurements were performed essentially in the thermal-wave regime with a relatively unfocused laser beam (spot size$\simeq$30 μm) and a relatively low-modulation frequency (100 kHz). The former condition means that the amplitude of the generated thermal wave is not optimum while the latter contributes to an increase in the thermal diffusion length and, thus, an increase in the signal integration depth in the material, well beyond the thickness of the implanted layer. Clearly, both of these factors contribute to our reduced sensitivity. Owing to our working in the thermal-wave regime, we are sensitive to thermal parameters that are primarily functions of phonon excitations of the lattice; recently, Opsal[27] has argued that it is advantageous to work in the plasma-wave regime (at modulation frequencies of $\sim$10 MHz), thus detecting plasma-wave effects, since the carriers are more sensitive to ion-implantation damage than phonons. Thus, our sensitivity to the implant dose could be improved by decreasing the spot sizes of the two laser beams and by increasing the modulation frequency, but the present experimental arrangement is optimal for decoupling and monitoring the temperature dependence of the thermal-wave PTR signal. An additional advantage of this arrangement is the validation of the one-dimensional (1D) theory of Sec. II for beam sizes larger than the damaged layer thickness, and the effective thermal diffusion length.

To examine the signal contribution of the crystalline substrate, consider the thermal diffusion length, μ_{th}, which is defined as

$$\mu_{th}(f,T)=\sqrt{\frac{k(T)}{\pi f\rho C(T)}}, \tag{6}$$

where the slight T variation of the silicon density has been suppressed ($\rho = 2.33$ g/cm^2 for c-Si).[22] The pronounced temperature dependence of μ_{th} suggests a new way to achieve depth profiling capabilities: in the case of the implanted wafers, the thermal properties of the bulk crystalline material may be playing a role, thereby diminishing the contribution of the damaged layer and making the corresponding PTR-T signals more similar to that of c-Si. The influence of the crystalline substrate is likely to decrease with increasing temperature, as the thermal diffusion length is largest at low T. We demonstrate the temperature dependence of μ_{th} of c-Si in Fig. 5(a), in the frequency range of 10–4000 kHz. Thus, with a typical implant depth of about 0.4 μm, the substrate contribution may become significant, especially at low temperatures. This hypothesis is borne out by the fact that the three curves of Fig. 4 seem to converge as the temperature is decreased.

In order to explain the temperature behavior of the PTR signal observed in Fig. 4, we examine the temperature behavior of the thermal-wave theory as summarized by Eq. (3). Figure 5(b) depicts the temperature dependence of the term $1/\sqrt{k\rho C}$ for crystalline silicon. Except at low temperatures, there is good qualitative agreement between the experimental results of Fig. 4 and the thermodynamic model predictions of Fig. 5(b). The discrepancy at very low T may have to do with the fact that the plasma-wave effects are beginning to contribute as the carrier lifetime increases with decreasing temperature.

To further test the validity of the proposed thermal-wave model, we studied the PTR-T response of an amorphous silicon film deposited on a crystalline substrate. This was done because the temperature dependence of the a-Si thermal conductivity exhibits opposite trends to that of

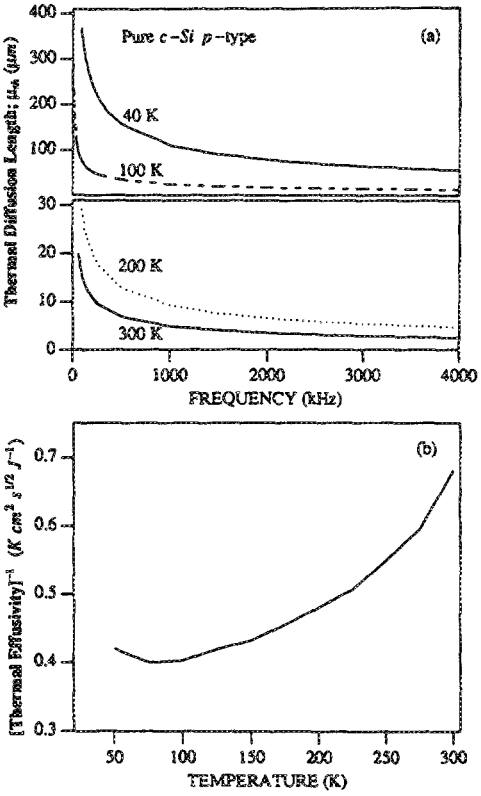

FIG. 5. (a) Thermal diffusion length, μ_{th} [from Eq. (6)], as a function of modulation frequency, for four different temperatures (crystalline c-Si). (b) thermal effusivity as a function of temperature (from Ref. 21).

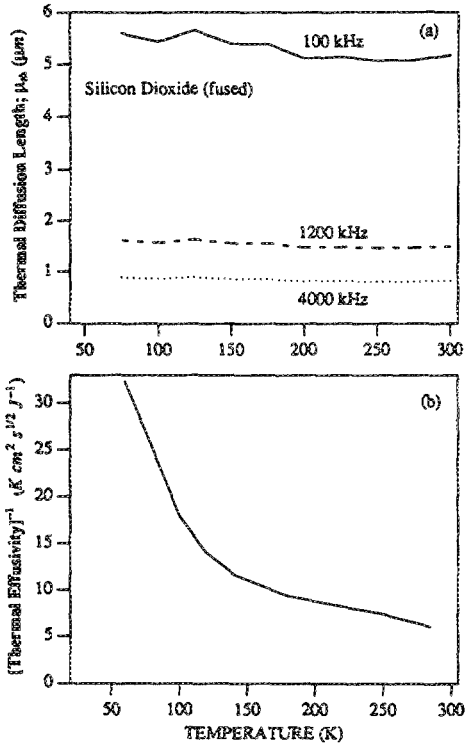

FIG. 6. (a) Thermal diffusion length, μ_{th} [from Eq. (6)], as a function of temperature, for three different modulation frequencies (silicon dioxide-fused). (b) thermal effusivity as a function of temperature (from Ref. 21).

c-Si, whereas the specific heat behavior of the two is similar. We approximated the thermal properties of a-Si by those of fused SiO_2, which are more readily available and are very similar, according to the literature.[21] The relevant thermal quantities of a-Si are shown in Figs. 6(a) and 6(b). As the thickness of our film was approximately 0.15 μm, we increased the modulation frequency in order to minimize the influence of the substrate. Figure 7 shows the observed results obtained at three different modulation frequencies. At $f = 4$ MHz, the limit of our sine-wave generator, the thermal diffusion length is much smaller than at 100 kHz, and the beam mainly samples the thermal properties of the amorphous silicon film. Therefore, the PTR signal decreases slightly with T, consistent with the trend depicted in Fig. 6(b). As the frequency is lowered, the crystalline substrate contribution should increase. This is reflected by the fact that at all but the highest frequency, the PTR signal tends to increase with T, the same behavior which was observed for the bulk c-Si. Once again, the plasma contribution to the modulated reflectance may be non-negligible in the MHz regime, and its temperature dependence could explain some of our observations; but qualitative agreement with the thermal wave model suggests that, at least to first order, the plasma effects are not playing a major role in our experiments.

In order to ensure that the thermal diffusion length does not exceed a given layer thickness, one may have to use prohibitively high-modulation frequencies. For example, an ion-implanted and subsequently annealed layer of 0.5 μm (with approximately c-Si-like thermal properties) would require a frequency of 110 MHz at room temperature in order to fully exclude the contribution of the substrate. Under such circumstances, the signal will likely be too small to be detected (see Fig. 3); however, as the $\mu_{th}(T)$ for crystalline silicon indicates, we may choose to raise the sample temperature and use more acceptable lower frequencies to achieve the same thermal diffusion length in the implanted film. This again hints at the depth profiling capabilities of the PTR-T method. The applicability to a layer of a given composition will be a strong function of its temperature-dependent thermal properties. This can be seen from the comparison of Figs. 5(a) and

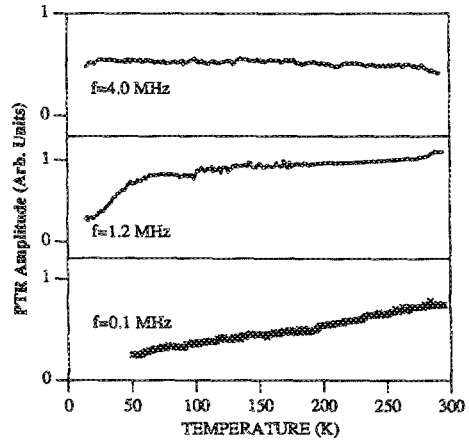

FIG. 7. PTR signal vs temperature for amorphous silicon sample at three different modulation frequencies (100, 1200, and 4000 kHz).

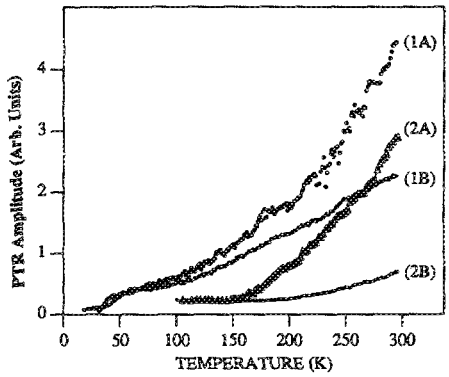

FIG. 8. Photothermal signal as a function of temperature for p-type c-Si and phosphorus-implanted silicon at two different modulation frequencies (1A = implanted, 3 kHz; 1B = implanted, 100 kHz; 2A = c-Si, 3 kHz; 2B = c-Si, 100 kHz).

6(a), which indicate that temperature depth profiling may be possible for the former, but not for the latter.

To see whether pure thermal-wave behavior was obtained for the crystalline p-type wafer analyzed in conjunction with Fig. 4, additional studies of this and a heavily damaged sample at a lower-modulation frequency $f = 3$ kHz were performed, thus limiting the relative importance of the plasma wave contribution. The experimental results are displayed in Fig. 8. The similarity of the temperature dependence of each pair of curves at the same frequency (trends and slopes) suggests that a given single mechanism is varying with lattice temperature, which, at these modulation frequencies and with widely varying carrier lifetimes, appears to be the one corresponding to the thermal-wave effect. Thus, it seems that at least to first order, no serious discrepancy is introduced by not invoking the plasma-wave effect described by Eq. (4).

We now present some results of PTR-T studies of silicon damaged by ion implantation. The effect of different annealing temperatures on the amplitude of the PTR signal of several highly doped samples (5×10^{14} As^+/cm^2) is depicted in Fig. 9. In general, the process of annealing is

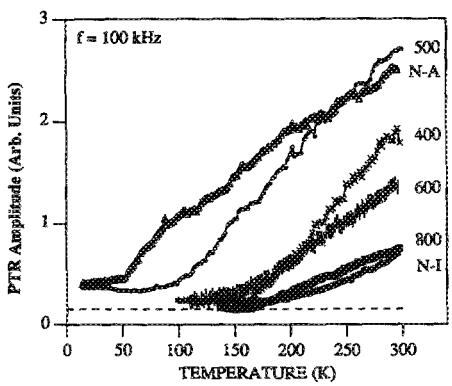

FIG. 9. Variation of PTR signal as a function of temperature for nonannealed and annealed samples (1 h) at annealing temperatures between 400 and 800 °C ($\Phi = 5\times10^{14}$ As^+/cm^2). N-A: nonannealed; N-I: nonimplanted.

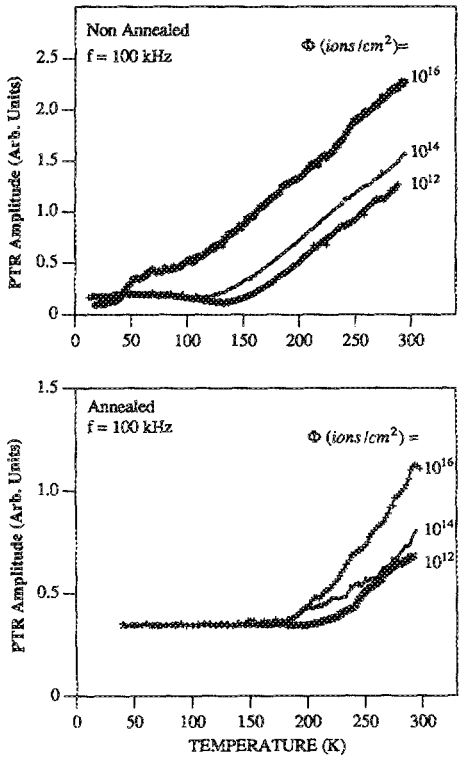

FIG. 10. PTR signal as a function of temperature for different samples implanted with phosphorus at different doses (nonannealed, and annealed at 1100 °C for 15 min).

thought to decrease the degree of local disorder, and thus cause a decrease in the locally induced temperature rise because of the average improvement of the sample parameters. In addition, annealing will decrease the optical absorption coefficient, thereby decreasing the amount of light energy absorbed at the surface. As Eq. (1a) indicates, a lower ΔT will reduce the magnitude of the thermal-wave effect, which, as shown above, seems to be the dominant mechanism of the PTR signal generation in our experiments. For higher annealing temperatures, the signal approaches that of the nonimplanted silicon, indicating a high degree of crystallinity restoration, as was observed previously using electrical methods such as Hall-effect and resistance measurements.[28] The phenomenon of negative annealing,[20] attributed to the formation of complex arsenic defects, is also observed in the annealing temperature range of 400–500 °C. The increasing signal intensity as a function of the measurement temperature for a given wafer can again be related to the average degradation of the thermal properties of the near-the-surface region (lower thermal conductivity, higher specific heat, higher nonradiative recombination rate, etc.). Once again, we note that at this modulation frequency (100 kHz) the free-carrier effect may be present in some of the well annealed samples (and in the nonimplanted sample), but the similar trend displayed by all the curves (except the anomalous range data, 400 and 500 °C curves) suggests that the temperature dependence can be explained in terms of the thermal-wave effect alone.

Figure 10 shows the PTR-T as a function of phospho-

rus dose, for as-implanted, and implanted and annealed silicon wafers. Lattice temperature dependencies similar to those observed and described in Fig. 9 are clearly seen. The relationships between various room-temperature amplitudes, which can be explained in terms of self-annealing behavior and thermal annealing kinetics, have been treated in detail in the companion paper.[9] Here, we simply note the increasing signal intensity with measurement temperature, in accordance with the foregoing theoretical considerations.

Finally, we must address the optical interference effects which have been detected previously in high-dose samples where the damaged surface layer and the underlying crystalline substrate form a clearly defined interface.[27,29] The interference fringes will be seen if the thickness of the damaged layer varies on the order of half the probe beam wavelength (for example, this thickness variation may be achieved by implanting at different energies at a fixed dose). In our experiments, we need to determine whether the thermal expansion effects could sufficiently change the thickness of the damaged layer as the temperature drops from 300 to 20 K. Using $l^{300\ \mathrm{K}} \approx 0.4\ \mu\mathrm{m}$ and the Si data presented by Touloukian,[21] we obtain $\Delta l^{20-300\ \mathrm{K}} \approx -0.009\ \mu\mathrm{m}$. Such a small thickness variation is not sufficient to give rise to an interference fringe, in agreement with our PTR-T results.

V. CONCLUSIONS

In this paper, we have examined the temperature variation of the PTR thermal wave signal from various silicon samples. The observed results have been semiquantitatively explained in terms of the T dependence of the thermal-wave effect alone. The variation of the thermal diffusion length with temperature, its effect on the PTR-T signal, and some possible applications to T-depth profiling have been discussed. Experimental results of PTR-T investigation of ion-implanted silicon have also been presented.

The main conclusions of our study can be summarized as follows:

(1) There is a strong variation of the photothermal signal with measurement temperature.

(2) The thermal-wave model has been extended to include the dependence of sample parameters on temperature, and has been proven successful in accounting for observed trends in the experimental data. To first order, given the focusing conditions and the range of modulation frequencies, the temperature dependence of the plasma-wave effect has not been seen to contribute significantly to the signals, and thus has been ignored.

(3) Contributions of the subsurface material to the PTR-T signal have been detected, and explained in terms of the frequency and temperature dependence of μ_{th}. This suggests some depth profiling applications as a function of experimental temperature.

(4) The PTR-T technique may become a useful tool in elucidating the thermal and optical phenomena in ion-implanted silicon; useful comparisons with results from experiments involving carrier transport may be drawn *vis-à-vis* the effects of implantation damage on carrier- and phononlike properties in semiconductors.

In fact, the transport properties of crystalline semiconductors are relatively well interpreted by the classical transport theories. Amorphous semiconductors have also been the object of several theoretical papers which are fairly successful in explaining their transport mechanisms in a qualitative way. On the other hand, it is difficult to interpret the transport properties of intermediary materials, namely inhomogeneous materials, which are complex hybrids of completely crystalline and amorphous materials. Implanted and nonannealed, or insufficiently annealed silicon layers are typical of these inhomogeneous materials; a characterization technique that provides useful information about the underlying processes in these complex materials can be an invaluable tool in constructing and verifying a quantitative model of their behavior.

ACKNOWLEDGMENTS

The authors wish to thank Dr. H. Jaouen and Mrs. Joumana of the Laboratoire PCS (ENSERG, Grenoble, France), and Dr. H. Naguib of Northern Telecom Electronics (Northern Telecom, Ottawa, Canada) for supplying the ion-implanted samples. Thanks are also due to Dr. S. Zukotinsky for providing us with useful references about the material properties of silicon. The support of the Ontario Laser and Lightwave Research Center is gratefully acknowledged.

[1] A. Rosencwaig, J. Opsal, W. L. Smith, and D. L. Willenborg, Appl. Phys. Lett. **46**, 1013 (1985).
[2] M. A. Olmstead, N. M. Amer, S. Kohn, D. Fournier, and A. C. Boccara, Appl. Phys. A **32**, 141 (1983).
[3] J. Opsal, A. Rosencwaig, and D. L. Willenborg, Appl. Opt. **22**, 3169 (1983).
[4] S. Ameri, E. A. Ash, V. Neuman, and C. R. Petts, Electron. Lett. **17**, 337 (1981).
[5] P. E. Nordal and S. O. Kanstad, Infrared Phys. **25**, 295 (1985).
[6] A. C. Tam, *Photoacoustic and Thermal Wave Phenomena in Semiconductors*, edited by A. Mandelis (North-Holland, New York, 1987), p. 175.
[7] W. L. Smith, A. Rosencwaig, and D. Willenborg, Appl. Phys. Lett. **47**, 584 (1985).
[8] D. Guidotti and H. M. van Driel, Appl. Phys. Lett. **47**, 1336 (1985).
[9] C. Christofides, I. A. Vitkin, and A. Mandelis, J. Appl. Phys. **67**, 2815 (1990).
[10] I. A. Vitkin, C. Christofides, and A. Mandelis, Appl. Phys. Lett. **54**, 2392 (1989).
[11] J. Opsal, M. W. Taylor, W. L. Smith, and A. Rosencwaig, J. Appl. Phys. **61**, 240 (1987).
[12] A. Rosencwaig, *Photoacoustic and Thermal Wave Phenomena in Semiconductors*, edited by A. Mandelis (North-Holland, New York, 1987), p. 97.
[13] F. A. McDonald, D. Guidotti, and T. M. DelGuidice, IBM Internal Report No. 54561 (April, 1986).
[14] B. G. Streetman, *Solid State Electronic Devices*, 2nd ed. (Prentice-Hall, New York, 1980), Chap. 4.
[15] A. Mogro-Campero and R. P. Love, *Thirteenth International Conference on Defects in Semiconductors*, edited by L. C. Kimerling and J. M. Parsey, Jr. (Metallurgical Society, Pennsylvania, 1985), p. 565.
[16] D. Guidotti and H. M. van Driel, Appl. Phys. Lett. **49**, 301 (1986).
[17] G. C. Wetsel, Jr., IEEE Trans. Ultrason. Ferroelectr. Freq. Control **UFFC-33**, 450 (1986).

[18] O. Doka, A. Mikos, and A. Lorincz, J. Appl. Phys. **63**, 2156 (1988).
[19] T. Tomita, T. Kinosada, T. Yamashita, M. Shiota, and T. Sakurai, Jpn. J. Appl. Phys. **25**, L925 (1986).
[20] J. F. Gibbons, Proc. IEEE **60**, 1062 (1972).
[21] Y. S. Touloukian, Series Ed., *Thermophysical Properties of Matter*, Vol. 1 (Plenum, New York, 1970), p. 326.
[22] S. M. Sze, *Physics of Semiconductors Devices* (Wiley-Interscience, London, 1969), Chap. 2.
[23] K. Ishikawa, M. Yoshida, and M. Inoue, Jpn. J. Appl. Phys. **26**, L1089 (1987).
[24] W. L. Smith, A. Rosencwaig, D. L. Willenborg, J. Opsal, and M. W. Taylor, Solid State Technol. **29**, 85 (1986).
[25] B. J. Kirby, L. A. Larson, and R. Liang, Nucl. Instrum. Methods B **21**, 550 (1987).
[26] J. Schuur, C. Waters, J. Maneval, N. Tripsis, A. Rosencwaig, M. W. Taylor, W. L. Smith, L. Golding, and J. Opsal, Nucl. Instrum. Methods B **21**, 554 (1987).
[27] J. Opsal, Sixth International Conference on Photoacoustic and Photothermal Phenomena (Baltimore, MD, 1989), paper WPm20; and private communication.
[28] C. Christofides, G. Ghibaudo, and H. Jaouen, Rev. Phys. Appl. **22**, 407 (1987).
[29] S. Wurm, P. Alpern, D. Savignac, and R. Kakoschke, Appl. Phys. A **47**, 147 (1988).